Pure Appl. Chem., Vol. 77, No. 6, pp. 977–993, 2005.
DOI: 10.1351/pac200577060977

Toward a computational photobiology*

Adalgisa Sinicropi[1], Tadeusz Andruniow[1,2], Luca De Vico[1], Nicolas Ferré[3], and Massimo Olivucci[1,‡]

[1]Dipartimento di Chimica, Università di Siena, Italy; [2]Department of Chemistry, Institute of Physical and Theoretical Chemistry, Wroclaw University of Technology, Wroclaw, Poland; [3]Laboratoire de Chimie Théoretique et de Modélisation Moléculaire, CNRS Université de Provence, France

Abstract: In this paper, we discuss the results of our recent studies on the molecular mechanism, which stand at the basis of the photochemical processes occurring in photobiological systems. These results are obtained using modern, robust, and fairly accurate high-level quantum chemical methods.

Keywords: photobiology; computational photobiology; quantum chemical; molecular mechanisms; photoisomerization.

INTRODUCTION

The aim of this contribution is to show that computers can now be used to understand the molecular mechanism of photochemical processes occurring in photobiological systems. Accordingly, we discuss some recent spectral simulations of the visual pigment rhodopsin (Rh) and of the green fluorescent protein (GFP). We also present work related to the mapping of the photoisomerization path of these complex bioorganic molecules.

In simple terms, there are two events that may happen when the light energy is absorbed by a molecule. This energy is either wasted or exploited (Scheme 1). The control of these events can be considered as a basic requirement for the rational design of efficient photochemical reactions, artificial photosynthetic systems, novel materials, molecular devices, and molecular-level machines. In fact, technology often requires molecules where this energy is not wasted, but exploited to achieve specific chemical, conformational, and electronic changes. In contrast, other applications, such as those in the fields of photoprotection or photobiology, need molecules that are structurally unaffected by light absorption (e.g., through light emission and internal conversion).

In this respect, during the last few years, computational methods have been successfully applied to explore energy wastage processes such as the quenching of fluorescent probes [1–3] and the mechanism of fast internal conversion in the photostabilization of DNA basis [4,5]. Similarly, as an example of process where light is exploited to drive efficient and stereoselective photochemical reactions, we can recall the ultrafast pericyclic reactions [6]. Most interestingly, the same types of processes are known in photobiology. For instance, there are fluorescent proteins, such as GFP, where the energy of the photon can be wasted to produce fluorescence, while there are other photoreceptors, such as the visual pigment Rh, where the energy of the photon is exploited to produce a change in the protein structure.

---

*Paper based on a presentation at the XXth IUPAC Symposium on Photochemistry, 17–22 July 2004, Granada, Spain. Other presentations are published in this issue, pp. 925–1085.
‡Corresponding author

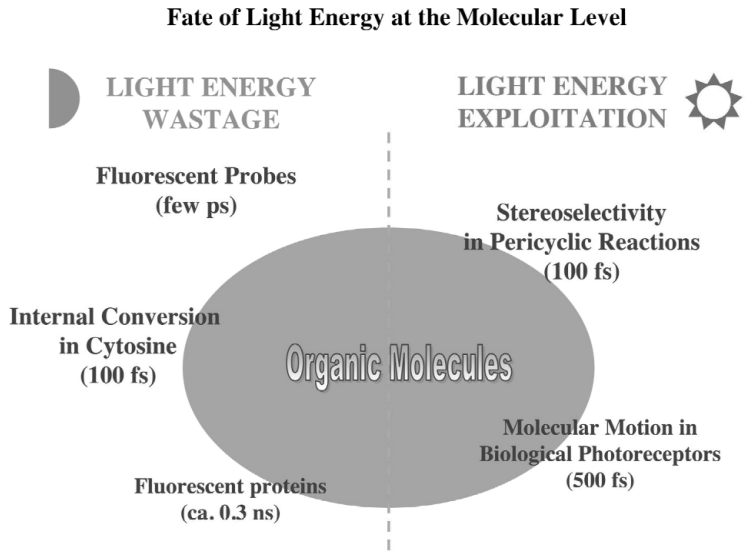

Scheme 1

Our approach to these types of mechanistic problems is that of computing the photochemical reaction path. As illustrated in Fig. 1, once species A is promoted to the excited state, it starts to evolve on the corresponding potential energy surface (PES). As a consequence of such relaxation, which may involve the overcoming of a transition state (TS), the species reaches a point of conical intersection (CI) and decays. The whole process can be described by computing a minimum energy path (MEP) starting at the Franck–Condon (FC) point (i.e., at the ground-state equilibrium structure) and ending at the CI. The CI provides a key mechanistic entity for the description of a photochemical reaction, and it can be seen as a very efficient channel for the decay to the ground state that, in the past, has been referred to as the photochemical funnel [7,8]. The photochemical funnel corresponds to a molecular structure that

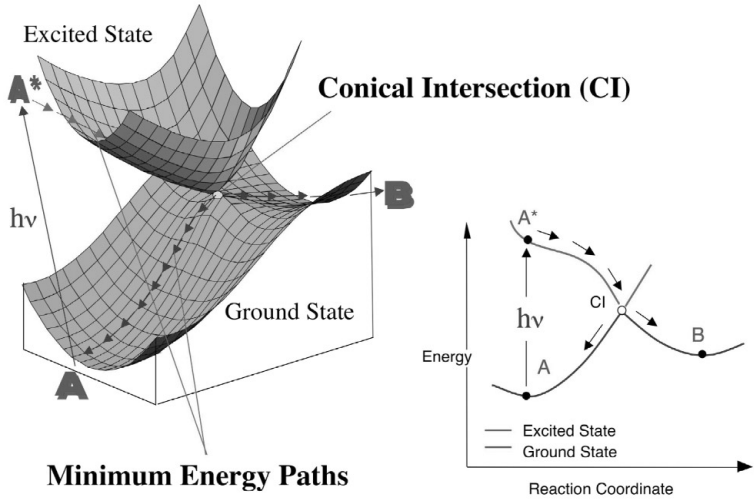

Fig. 1 Left side: Model intersecting the ground- (S_0) and the excited-state (S_1) PESs. The FC point (A*) is geometrically identical to the minimum on the ground state, but located on the S_1 surface. The arrows indicate the direction of the MEP connecting the FC point (A*) to the CI and then to A and the photoproduct B. Right side: a different schematic representation of the model on the left side.

lives for only a few femtoseconds (10^{-15} s). For this reason, computer simulations based on modern quantum chemical methods appear to be the only practical source of information. For a complete description of the reaction, we need to compute also the MEP on the ground state that describes photoproduct formation. In Fig. 1, we show that the entire photochemical reaction path is defined and computed in terms of a set of connected MEPs. In particular, the path starting at the FC (structure A*****) on the PES of the spectroscopic excited state and ending at the photoproduct energy minimum B located on the ground-state energy surface is constructed by joining two MEPs. The first MEP (gray arrows) connects the FC point to the CI (A* → CI). The second MEP (black arrows) connects the CI to the photoproduct (CI → photoproduct B). One can also compute a third MEP that starts at the CI and describes the reactant reconstitution process (CI → A) responsible for partial return of the photoexcited species to the original ground-state minimum. As described below, this mechanistic scheme is very general.

The nature of the CI has been a subject of research for at least three decades. Between 1966 and 1972, Zimmerman, Michl, and Salem [9–14] were the first to propose, independently, that for a broad class of organic reactions the structure of the funnel could be determined by locating a "cone-shaped" crossing of the excited and ground-state (potential) energy surfaces, known as CI.

At the end of the 1980s, improved quantum chemical methods and faster computers became available which were suitable for computing excited-state energy surfaces. In 1990, Olivucci, Bernardi, and Robb [15,16] used these methodologies to explain the photochemical cycloaddition of ethylene: both a vital material for the chemical industry and a plant hormone. It was shown that

i a CI exists right at the bottom of the excited-state energy surface of two interacting ethylene molecules, and
ii the molecular structure of the CI was intimately related to the observed production of cyclobutane, a hydrocarbon which is square in shape.

These initial results suggested that CIs could indeed act as photochemical funnels.

Since there is no general theorem supporting the existence of low-lying CIs in organic molecules, the only way to prove the general validity of the hypothesis above was a painstaking systematic search for properties i–ii in different classes of organic molecules. Thus, in 1992 Olivucci and Bernardi in Bologna and Robb in London started a long-term computational project.

The excited energy surface of ca. 25 different organic chromophores was mapped to search for CIs [17]. The examination of a large set of computed data allowed the formulation of a few general results that lie at the basis of the "chemistry" of CIs:

- Similar organic chromophores (e.g., conjugated hydrocarbons) have similar CI structures.
- All basic chemical events such as breaking, making, and exchange of bonds between atoms can potentially be mediated by CIs.

Computational tools and strategies have been developed to tackle the problem of determining the molecular structure and energy of mechanistically relevant CIs. These tools have the ability to

- trace the excited-state MEP starting from the FC point (i.e., the ground-state equilibrium structure of the system A* in Fig. 1) or from an excited-state reactant and ending at a CI or excited-state intermediate;
- locate the lowest energy CI for a given, initial, molecular structure; and
- determine the possible initial (steepest) relaxation directions starting from the located CI and follow the associated MEPs connecting the intersection to the primary photoproduct energy minima.

FATE OF LIGHT ENERGY IN PHOTOBIOLOGY

In this work, we use computational photochemistry methods to investigate two very different spectroscopic problems. The first problem regards the GFP, a protein that can waste light energy with great ef-

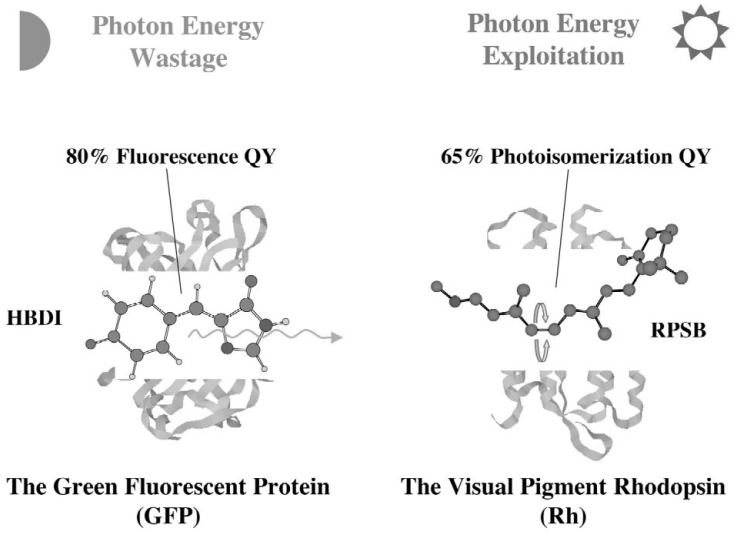

Fig. 2 Ball-and-stick representation of the GFP chromophore (left side) as an example of molecule that can waste the photon energy and of the visual pigment Rh chromophore (right side), which can efficiently convert the light energy into molecular motion.

ficiency through fluorescence (left side of Fig. 2). The second protein, the visual pigment Rh, is instead designed to exploit light energy to drive a double-bond photoisomerization reaction (right side of Fig. 2).

The GFP consists of a rigid β-sheet-based structure, and the prosthetic group that is responsible for the green fluorescence is the anionic form of a *p*-hydroxybenzilideneimidazolone (HBDI) located at the center of the barrel-like protein backbone (left side of Fig. 2). The fluorophore is excited by UV light and fluoresces with an 80 % quantum yield [18,19]. The Rh structure is totally different; it is more flexible, and is mainly characterized by an α-helix structure. The chromophore of the Rh is an 11-*cis* retinal chromophore (PSB11) bound to a lysine residue (Lys296) via a protonated Schiff base linkage (right side of Fig. 2). The chromophore undergoes a *Z*/*E* photoisomerization, which triggers the Rh activity [20,21]. Both the chromophores of GFP and Rh are ion pairs (see Fig. 3). In the case of GFP, HBDI anion is coupled to an Arg cation, while in the visual pigment the retinal PSB cation is interacting with a Glu113 carboxylate counterion.

The excited-state lifetime of the GFP chromophore is very long in the protein (ca. 3 ns), but much shorter (less than 0.3 ps) in solution. The mechanistic idea is that the decay is due to a *Z*/*E* isomerization, but while in the solution, the fluorophore basically undergoes an ultrafast internal conversion, the protein should act by restraining the isomerization. In deep contrast in the Rh protein, the excited-state lifetime is ca. 150 fs. However, if we look at the solution lifetime, this is increased by one order of magnitude. Furthermore, one has 24 % quantum yield in solution and 65 % quantum yield in protein. Thus, in this case, the protein is catalyzing the reaction.

The absorption maxima of the two proteins are also very environment-dependent. In fact, while the absorption of HBDI in solution is 426 nm, GFP has a much red-shifted (495 nm) absorption maximum. The same behavior has been found in Rh: the absorption of retinal is 442 nm in solution, and it becomes 498 nm in the protein. Why is this red shift inside the protein?

Before answering this question, we have to say a few words about quantum chemical technology.

Among the possible types of available quantum chemical technologies (e.g., semiempirical, DFT, and ab initio) one could use to compute the PES of an excited-state molecule, we adopt an ab initio CASPT2//CASSCF (complete active space/self-consistent field) approach. This is considered a "practical" compromise between computational cost and computational accuracy, as well as a robust quan-

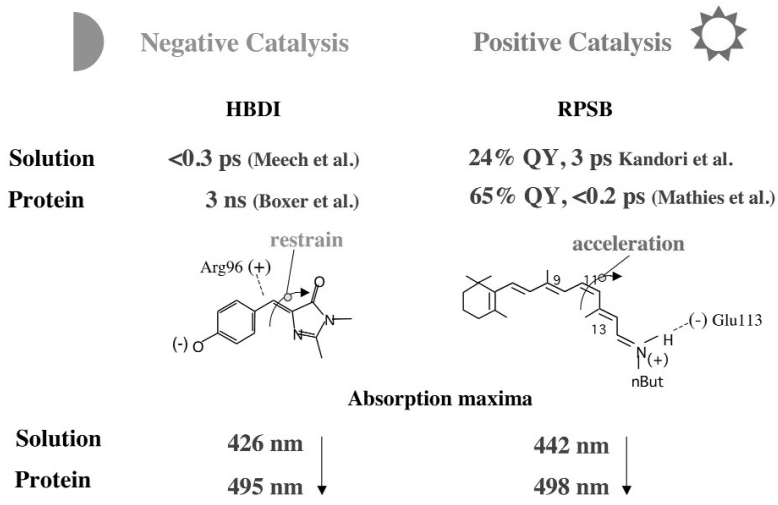

Fig. 3 Excited-state lifetimes, quantum yields, and absorption maxima for the GFP chromophore (left side) [22–24] and the visual pigment Rh chromophore (right side) [20,21] in different environments (solution and protein). These features contribute to explain the different behavior of the two proteins.

tum chemical strategy when comparison with observed spectroscopic quantities and reaction barriers are needed. In fact, the CASPT2 (i.e., an implementation of second-order multireference perturbation theory) level ensures a correct balance of dynamic and nondynamic electron correlation in the wavefunction. However, CASPT2 geometry optimizations [25] are presently not feasible even for medium-size organic molecules. Thus, in the CASPT2//CASSCF computations, the geometry and the reaction coordinate are computed at the CASSCF level of theory, while the associated energy profile (determining the reaction energetics) is reevaluated along a selected series of reaction coordinate points by performing single-point CASPT2 computations.

A step forward along the route to the correct modeling of spectroscopy and photochemical reactivity of photoreactive proteins is represented by the implementation of a quantum mechanics/molecular mechanics (QM/MM) computational strategy based on a CASPT2//CASSCF QM part coupled with a protein force field such as AMBER [26] or CHARMM [27]. Very recently, a CASPT2//CASSCF/AMBER method for Rh has been implemented in our laboratory [28,29] within the QM/MM link-atom scheme [30]. Special care has been taken in the parametrization of the protonated Schiff base linkage region that describes the delicate border region between the MM (the protein) and QM (the chromophore) subunits [29] (see Scheme 2). While below we review the results of this ab initio QM/MM method, other alternative approaches have been presented [31–39].

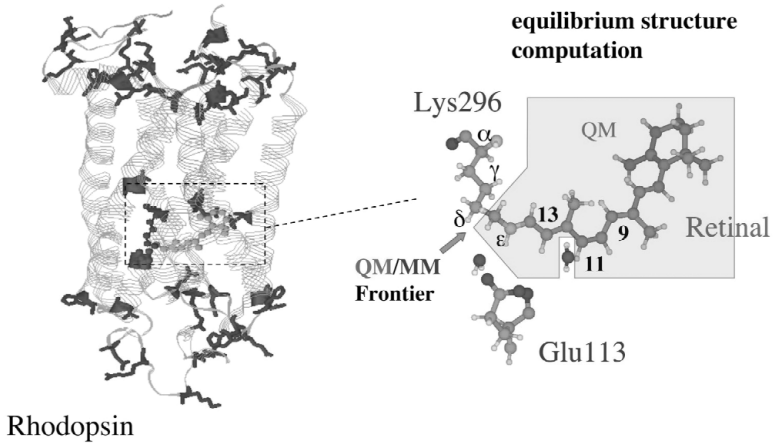

Scheme 2

GFP spectroscopy

The GFP chromophore is an important case since the gas-phase spectra of its fluorophore are available, and one can effort a direct comparison with the experiment in different environments (gas-phase, solution, protein matrix) [40,41]. This comparison is schematically reported in Scheme 3. Now, if one looks at the absorption in the protein and in solution, it is clear that the gas-phase absorption maximum is substantially closer to the protein absorption maximum than to the solution absorption maximum. This suggests a rather naïve idea that the GFP protein cavity offers an environment more similar to the gas phase than to the solution.

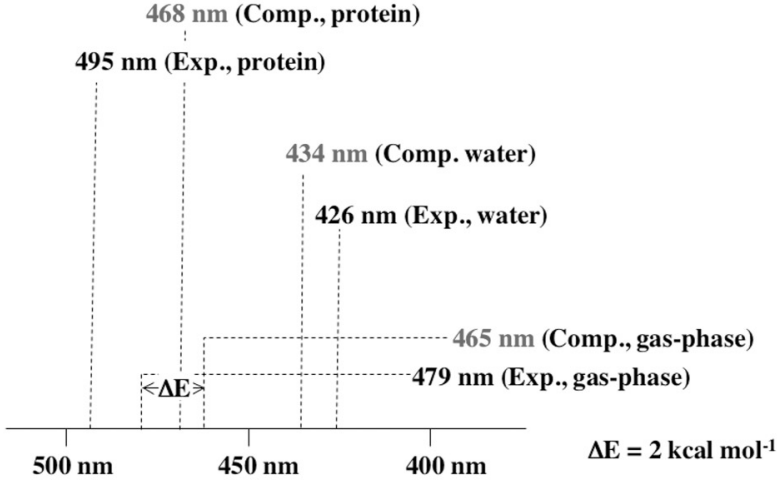

Scheme 3

The absorption maxima simulation correctly reproduces the closeness of the gas-phase and protein absorption λ_{max}. Geometry optimizations in the different environments indicate that the protein, gas-phase and solution spectral features are related to the nature of the chromophore structure. Notice that, remarkably, as shown in Fig. 4, the equilibrium structures in the protein (Fig. 4a) and in the gas phase (Fig. 4c), display close absorption maxima in spite of the different geometrical structures.

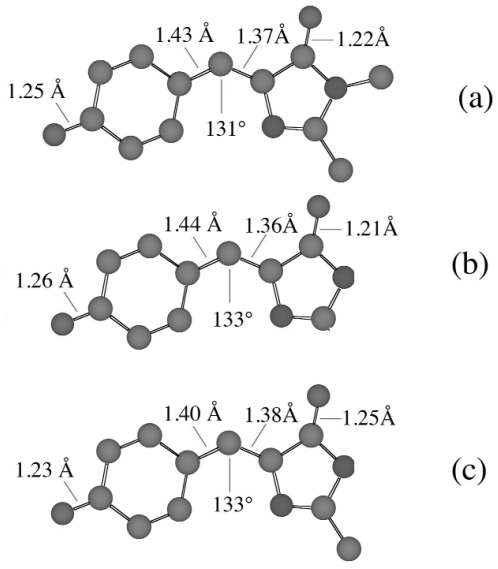

Fig. 4 Ground-state CASSCF optimized structures for the GFP chromophore in three different environments: (a) protein, (b) water solution, and (c) in vacuo. Geometrical parameters are in Å and degrees.

The CASSCF/AMBER method allows for geometry optimization on the excited state. Thus, we can also predict the emission maxima. The results, schematically illustrated in Scheme 4, indicate that the protein/gas-phase similarity also holds for the emission, suggesting that the protein matrix mimics the gas phase even for the relaxed excited-state chromophore.

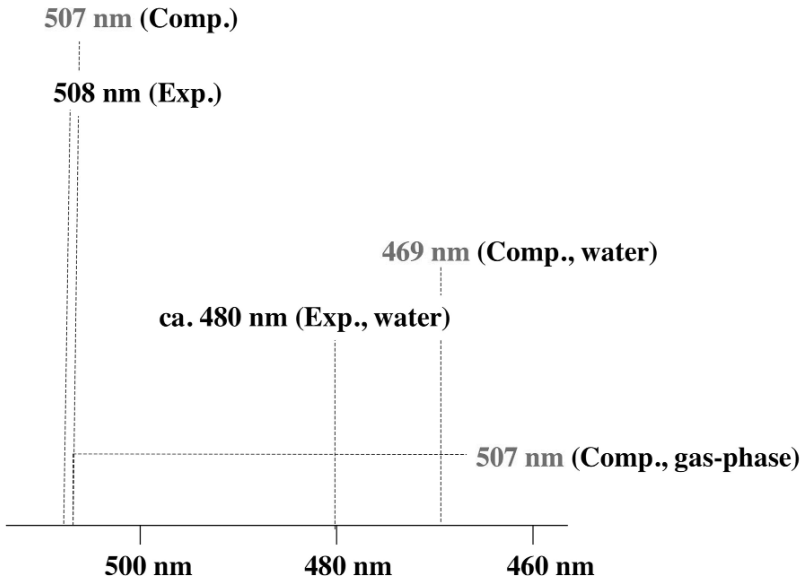

Scheme 4

Rh spectroscopy

As already mentioned at the beginning of the second section, the visual pigment Rh [20,21] is a G-protein-coupled receptor containing an 11-*cis* retinal chromophore (PSB11) bounded to a lysine residue

(Lys296) via a protonated Schiff base linkage (see dashed frame in the structure below). While the biological activity of Rh is triggered by the light-induced isomerization of PSB11, this reaction owes its efficiency (e.g., short timescale and quantum yields) to the protein cavity. Accordingly, the investigation of the environment-dependent properties of PSB11 is a prerequisite for understanding Rh "catalysis". The equilibrium geometry and absorption maximum (λ_{max}) are indicators of the environment effect.

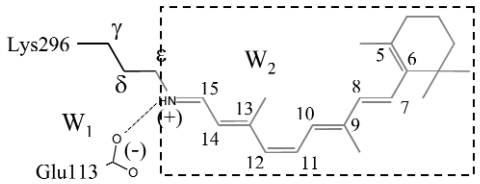

We have recently [28] provided evidence that our CASPT2//CASSCF/AMBER strategy can be correctly applied to the investigation of the excited state of Rh with a computational error <5 kcal mol^{-1}. Thus, our simulation allows for a semiquantitative analysis of the factor determining the properties of the protein environment. Comparing the computed vertical excitation energy with the experimental values (see Scheme 5), we found that for Rh the absorption maximum is reproduced with only 3 kcal mol^{-1} error (476 vs. 498 nm), while for the solution the error is only 1 kcal mol^{-1} (433 vs. 442 nm). These results confirm the quality of our approach and allow reproducing the so-called "opsin-shift" (the 445 nm λ_{max} observed for PSB11 in methanol is red-shifted to 498 nm in Rh) with a 2 kcal mol^{-1} error.

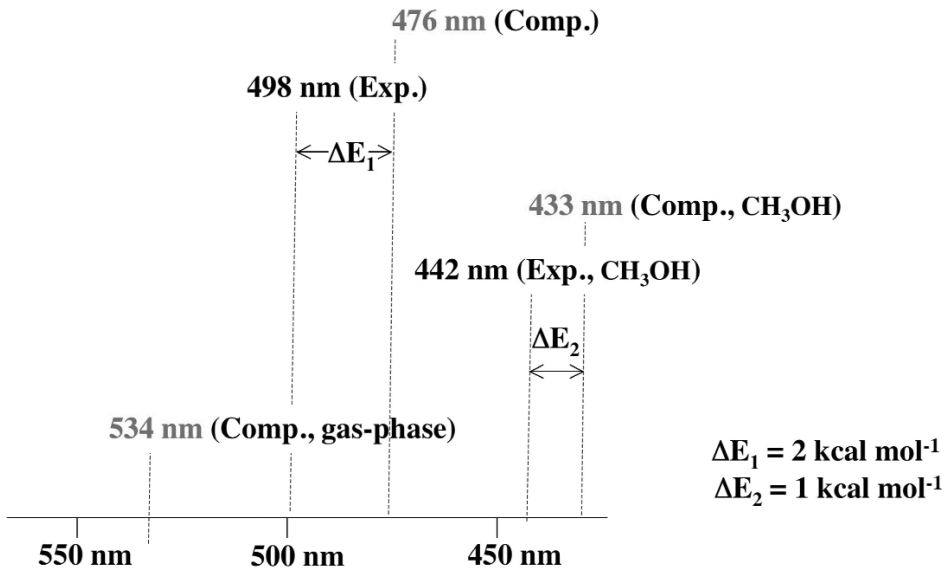

Scheme 5

As shown in Fig. 5, the S_0 Rh chromophore optimized structure (protein) is close to the crystallographic (X-ray) and NMR structures observed experimentally for bovine Rh. Comparing this geometry with the one obtained for PSB11 in methanol solution, using Cl^- as counterion, it is evident that the central segment of PSB11 is nearly planar and the β-ionone ring is 10° more twisted than in the protein.

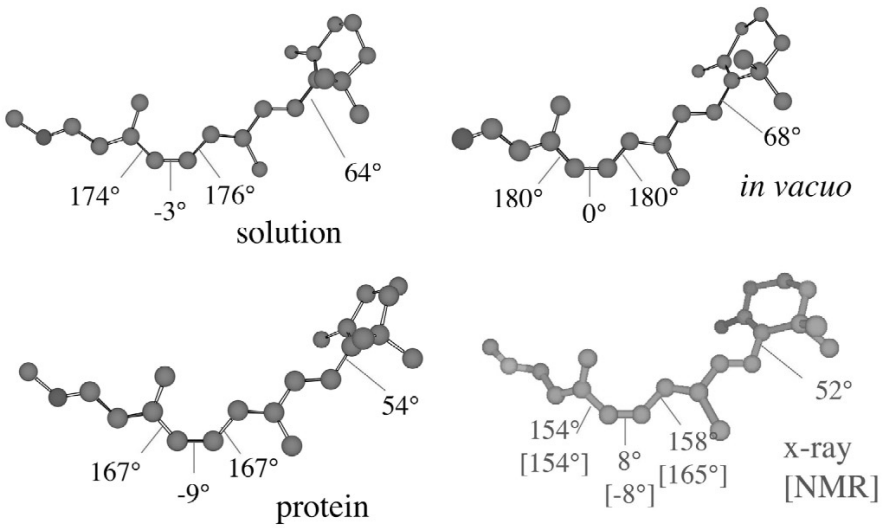

Fig. 5 Ground-state CASSCF optimized structures for the Rh chromophore in solution, in vacuo and in the protein compared to the crystallographic and NMR structure.

The excitation energy of the chromophore-counterion (Glu113) system (**RPSB + count.**, taken with its Rh geometry) is increased leading to a strongly blue-shifted λ_{max}. The isolated RPSB displays instead an absorption maximum much closer to that of the protein. The results, illustrated in Scheme 6 (adapted from ref. [28]), suggest that the protein matrix offsets or counterbalances the electrostatic effect of the counterion. The excitation energy in solution is more similar to the chromophore-counterion couple than to the protein, thus indicating that the offsetting effect of the solvent environment is less marked.

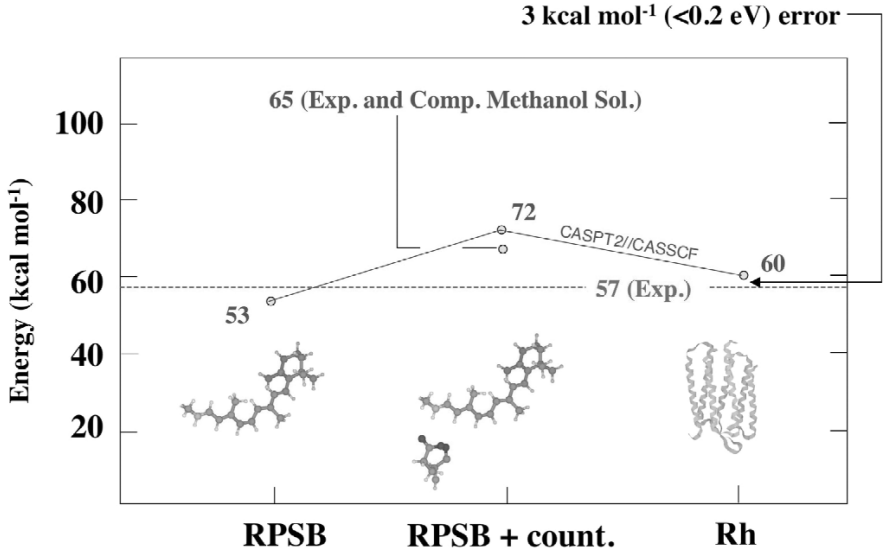

Scheme 6

Why is the counterion causing this effect? Quantum chemistry may help us to give an explanation. In fact, if one looks at the ground- and excited-state charges (Fig. 6), upon excitation there is a

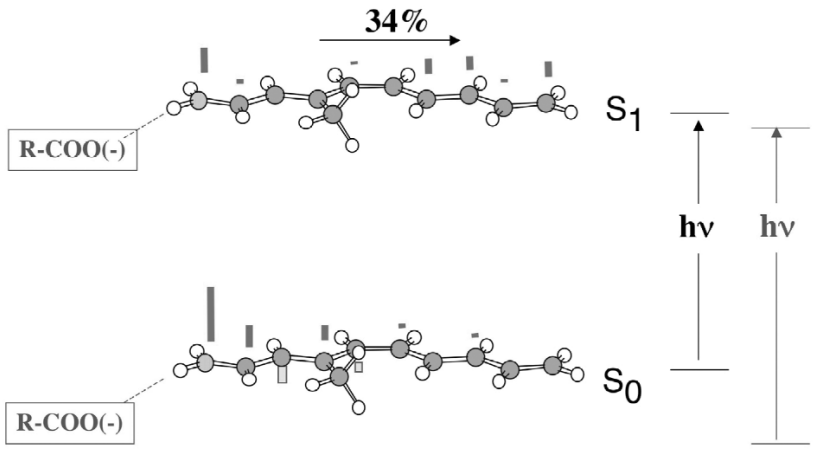

Fig. 6 Ground- and excited-state Mulliken charges along the backbone of Rh showing the displacement of the positive charge along the molecule and toward the C-end.

34 % (with respect to the center of the chain) displacement of the positive charge along the molecule and toward the C-end. When the counterion is close to the PSB, the Glu113 stabilizes preferentially the ground state (where the positive charge is located at the N-terminal) rather than the first excited state. This effect yields a larger S_1–S_0 energy gap, leading to the observed blue-shift. The specific charge distribution of the protein cavity counterbalances the effect of the counterion decreasing the S_1–S_0 energy gap.

Photoisomerization path of Rh

We have recently demonstrated that the same level of theory can be used to get realistic information on the excited- and ground-state relaxation of PSB11 in the Rh cavity or, in other words, to compute the entire photochemical reaction path [42,43]. This information will enable us to understand the mechanism driving the excited-state decay and photon energy storage in Rh. Time-resolved spectroscopy studies have established that a first transient species (see Fig. 7) is formed after 50 fs. This fluorescent intermediate (FS-Rh) features a λ_{max} in the range of 600–700 nm. A second transient species is detected after ca. 200 fs (photoRh). The first ground-state isolable intermediate is instead formed in 2 ps (bathoRh). In Fig. 7, we display the points located along the photochemical reaction path of Rh. We have located the excited-state structure corresponding to FS-Rh. Its energy is evalu-

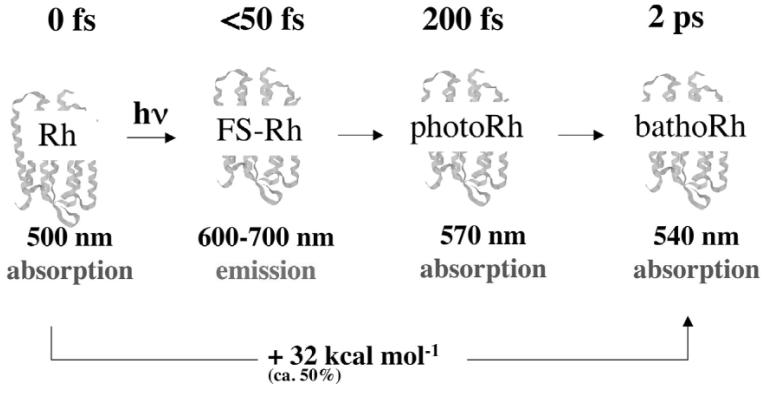

Fig. 7 Computed points along the photochemical reaction path of Rh.

ated to be 1 kcal mol^{-1} off the experimental value. Then we located the structure of the lowest-lying S_1/S_0 CI (CI-Rh), which corresponds also to the absolute S_1 minimum. This structure displays a ca. 90° twisted central C_{11}–C_{12} double bond. Starting at the CI geometry and via standard geometry optimization, it has been possible to locate the first stable ground-state intermediate (bathoRh) with 540 nm of absorption featuring an all-*trans*-like chromophore structure (about 150° twisted C_{11}–C_{12} double bond).

It has not yet been possible to unambiguously assign the photoRh transient that may well be a low-energy, excited-state or a high-energy, ground-state transient.

Concerning the energy storage problem (ca. 32 kcal mol^{-1} are efficiently stored in bathoRh), the results of our CASPT2//CASSCF/AMBER energy profile (Fig. 8) show that we are able to reproduce energy storage with an error of 5 kcal mol^{-1}.

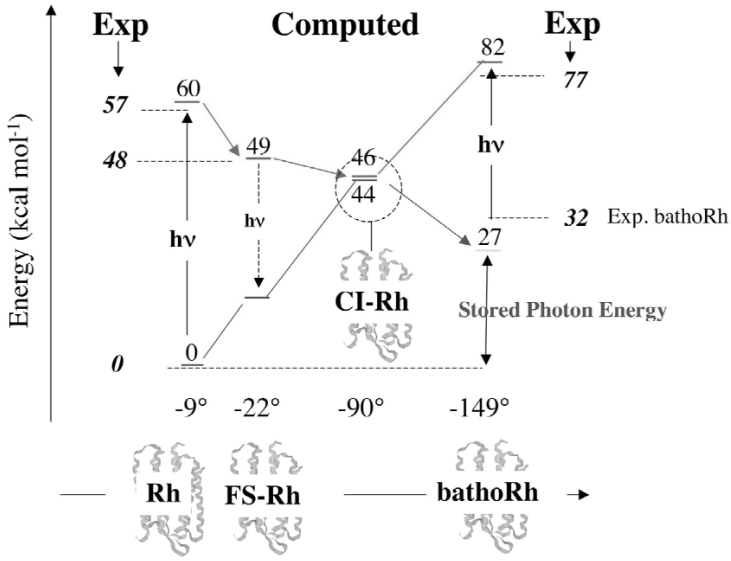

Fig. 8 CASPT2//CASSCF/AMBER energy profile for the Rh → bathoRh photochemical reaction compared to the experimental values (in bold). Redrawn with permission from ref. [42] © 2004 by The National Academy of Sciences of the USA.

What about the geometry evolution on the excited state? The change in the chromophore structure, occurring immediately after excitation, involves the bond lengths of the –C_9=C_{10}–C_{11}=C_{12}–C_{13}=C_{14}– moiety. In fact, at FS-Rh there is a complete inversion between single and double bonds (Fig. 9). The CI-Rh displays a highly helical structure compared to Rh and FS-Rh and is mainly characterized by large structural change in the –C_9=C_{10}–C_{11}=C_{12}–C_{13}=C_{14}– moiety. Thus, the motion driving the $S_1 \rightarrow S_0$ decay is mainly torsional with rotation of about 68° (22° → 90°) around the C_{11}=C_{12} bond and 37° and 15° twisting around the C_9=C_{10} and C_{13}=C_{14} bonds, respectively. In contrast to the initial excited-state relaxation, at CI all the other bonds remain substantially unchanged. Therefore, from a general point of view, during photoisomerization the structural changes do not occur exclusively at the central double bond, but also involve the other two adjacent double bonds, leading to a global change in the helicity of the chromophore.

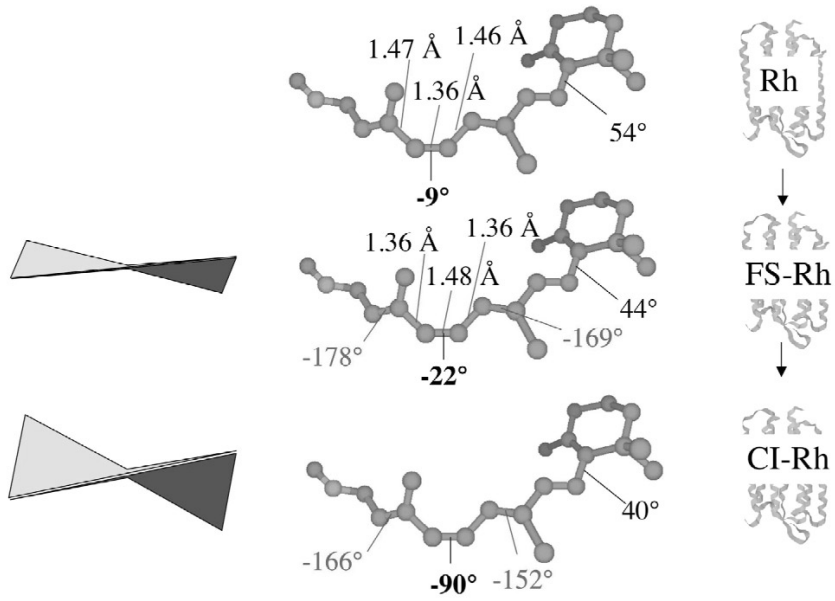

Fig. 9 Geometry evolution along the excited-state reaction path connecting Rh to CI-Rh. Adapted from ref. [42].

Nature of the energy storage

By decomposing the computed 26 kcal mol^{-1} stored photon energy in terms of a change in steric interaction between the chromophore and the protein cavity, we have seen that this accounts for only ca. 7 kcal mol^{-1}. This is consistent with the fact that the photoisomerization requires little displacement/reorientation of the PSB11 backbone. The superposition of bathoRh and Rh ground-state structures (Fig. 10) shows that the position of the PSB11 and β-ionone ring remains substantially unchanged while the structural change affects only the central fragment.

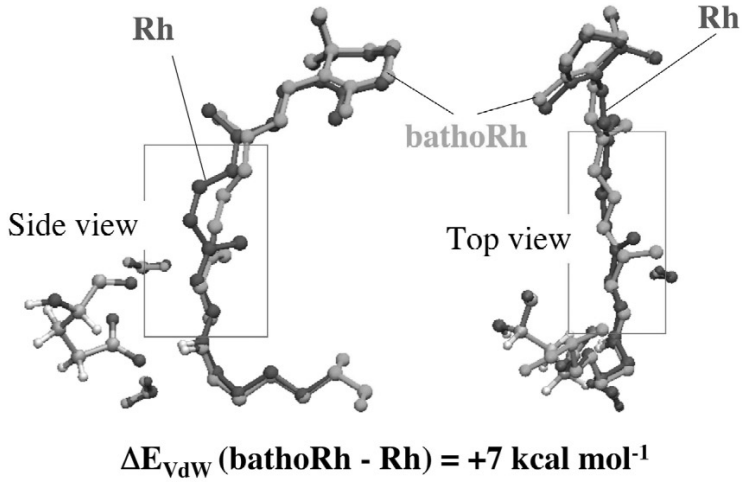

Fig. 10 Superposition of bathoRh and Rh structures. The frame indicates the part of the molecule that undergoes a structural change. Redrawn with permission from ref. [42] © 2004 by The National Academy of Sciences of the USA.

Since the calculated change in the electrostatic interaction between the chromophore and the protein cavity reveals a contribution of other ca. +6 kcal mol^{-1} (Scheme 7), the change in steric and electrostatic interaction must account for only half of the stored energy. So the photon energy has to be mainly stored in terms of the strain energy of the chromophore. In particular, it is due to the distorted π system of bathoRh (bond lengths and angles of the other moiety of the bathoRh are close to Rh) with respect to Rh.

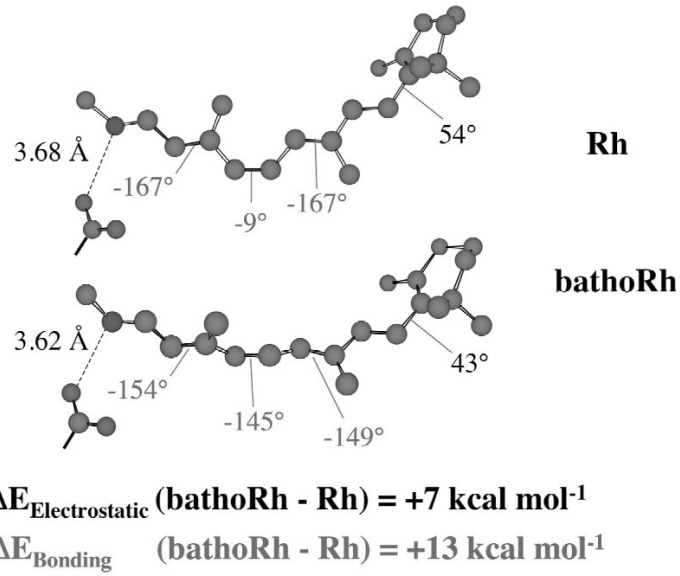

Scheme 7

In conclusion, the 32 kcal mol^{-1} photon energy stored in bathoRh are not fully related to a charge separation (a change in the electrostatic interaction between the chromophore and the protein cavity), but mostly "reside" in the highly strained chromophore of bathoRh where three different double bonds are not completely reconstituted.

Again, our conclusion is that three highly twisted double bonds in the first (isolable) intermediate bathoRh are responsible for ~50 % of the stored photon energy. The change in electrostatic and steric interaction of the chromophore with the protein cavity account each one for the 25 % of the stored energy.

FROM PHOTOBIOLOGY TO BIOMIMETIC MOLECULAR SWITCHES

Can what we have learnt from biology be used to design novel and more efficient light-driven molecular devices? In other words, can we design biomimetic photochemical switches that can exploit radiative energy to achieve a well-defined molecular structure deformation? The design, synthesis, and characterization of this type of molecular device appear to be of great importance in the field of modern technology such as the construction of light-powered nanodevices and, in particular, in the field of the conformational control of biopolymers [44–46]. In this last field, one can envision applications such as that of using light pulses to trigger protein folding/denaturation or to generate dynamical combinatorial libraries based on polypeptide backbones [47–49]. As an example of minimal biomimetic photochemical switches, we have recently studied the *trans–cis* photoisomerization of *N*-methylthioacetamide (NMTAA) [50] (see Scheme 8). Thio amino acids can in fact be integrated into the backbone of polypeptides without significantly perturbing their structure and can be excited selectively to induce

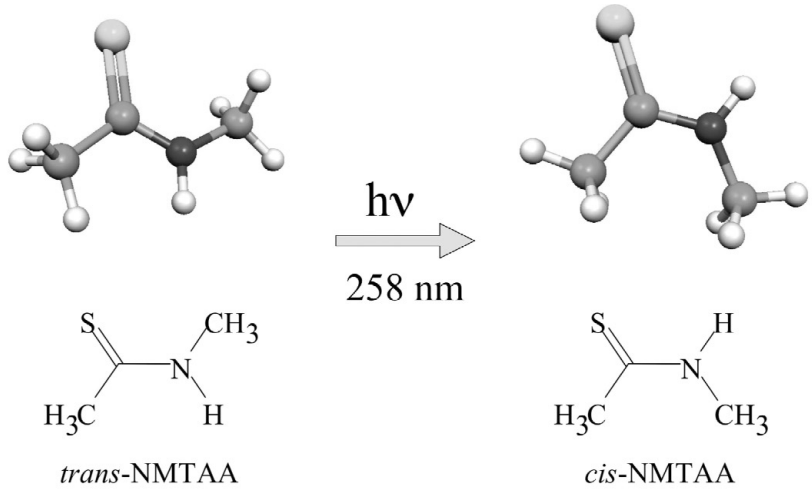

Scheme 8

a conformational change via *trans–cis* isomerization at a well-defined position in the peptide chain. The mechanistic scheme resulting from our investigation, combined with ultrafast spectroscopy experiments, show that the thio-photoswitch is photostable and potentially capable of inducing change with a high quantum yield on a subnanosecond timescale.

A more and fully efficient single-molecule switch may be found among molecules involved in photochemical reactions occurring on an ultrafast (i.e., picosecond or even subpicosecond) timescale and biological photoreceptors, such as retinal in Rh protein. Indeed, the photoisomeriztion of PSB11 can be seen as an extremely efficient single-molecule molecular motor due to the fact that the photoisomerization is stereoselective, unidirectional, and ultrafast and occurs with high quantum yield. Thus, molecules mimicking the PSB chromophore of Rh can be proposed as kinds of biomimetic switches.

In the present context, we are currently studying peptidomimetic polycyclic structure derived from the thioredoxin reductase active site [48,49], which consists of a domain of peptidic nature containing the sequence for the recognition and of a domain of nonpeptidic nature. In the present case, this last domain is formed by an unnatural amino acid of the size (i.e., isosteric) of a bi- or tri-peptide that can undergo *cis–trans* photoisomerization. Such isomerizations induce conformational changes in the peptide domain covalently attached to the motor mainly due to changes in the steric tension (angular or torsional). In general, such a ligand will have at least two tunable states. The tricycles system is shown in Scheme 9.

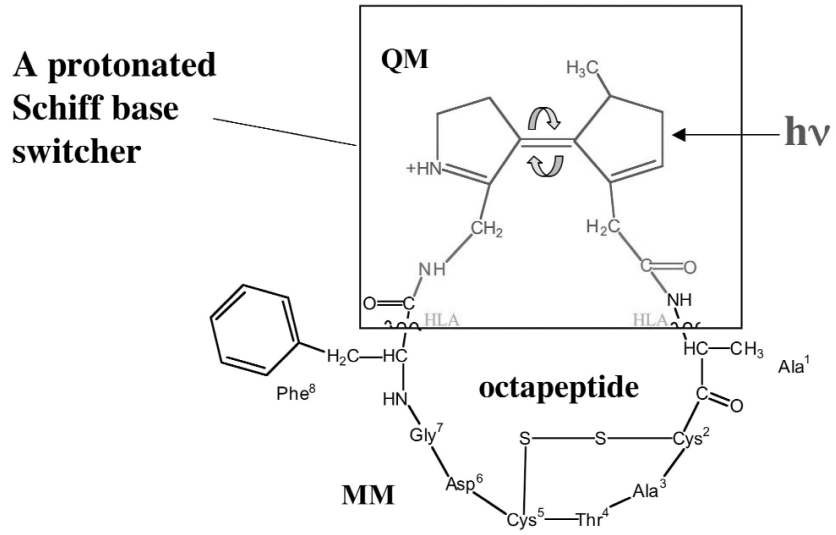

Scheme 9

The structure in blue represents the nonproteic domain. It is formed by a protonated Schiff base in which the isomerization of the two terminal double bonds are blocked by the inclusion of two five-membered rings. Such chromophore is rigid because of the presence of the central double bond and of the rings. Obviously, a light-triggered *cis–trans* isomerization in the switch will lead to remarkable conformational modifications in the peptide moiety. These conformational changes have been simulated using the same QM/MM method (CASPT2//CASSCF/AMBER) implemented in our laboratory [51]. The results of photochemical reaction path calculations for the whole system (in vacuo) show that the isomerization is driven by a nearly barrierless reaction path, and it is, in principle, an efficient process. The behavior of the switch is obviously biomimetic. The CI is 90° twisted as in the retinal chromophore. Along the excited-state reaction path, the oligopeptide structure does not change, but following the ground-state relaxation toward the *trans* form of the chromophore, the oligopeptide structure is largely modified. For example, the sulfur–sulfur bond, which is initially in a gauche conformation, is becoming anti. Similarly, the shape of the cyclic oligopeptide cavity is changing from bowl-like to elliptic.

A series of systems chemically similar to the chromophore shown in Scheme 9 have already been synthesized (Scheme 10) in our laboratory [52].

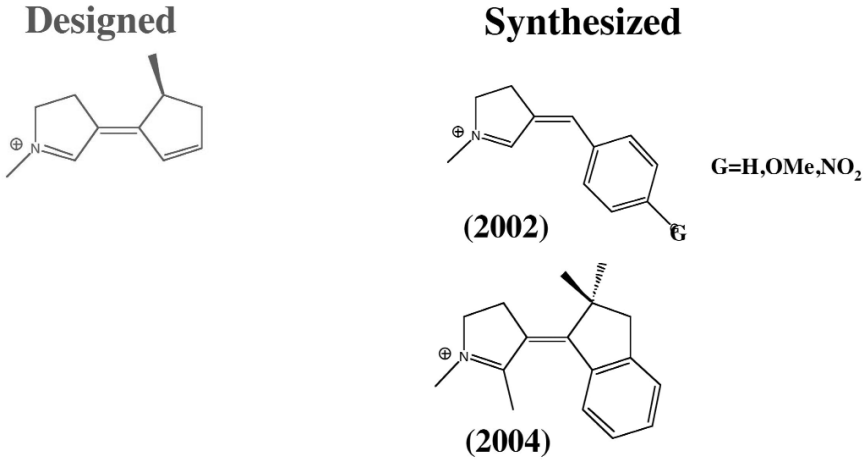

Scheme 10

CONCLUSIONS

We hope that we have provided some evidence that it is, nowadays, possible to investigate, at a semi-quantitative level, photobiological problems using computational tools. We have seen that using computer simulation we can potentially design new biomaterials inducing conformational changes in oligopeptides. We believe that these two complementary aspects of modern research in computational chemistry will become more and more important in the near future.

ACKNOWLEDGMENTS

Funds were provided by the Università di Siena (Progetto di Ateneo 02/04), FIRB project no. RBAU01EPRM and HFSP (RG 0229/2000-M). N. F. and T. A. are grateful for Marie Curie fellowships HPMF-CT-2001-01769 and HPMF-CT-2002-01769, respectively. We thank CINECA for granted calculation time.

REFERENCES

1. A. Sinicropi, U. Pischel, R. Basosi, W. M. Nau, M. Olivucci. *Angew. Chem., Int. Ed.* **39**, 4582–4586 (2000); ibid. *Angew. Chem*. **24**, 4776 (2000).
2. A. Sinicropi, R. Pogni, R. Basosi, M. A. Robb, G. Gramlich, W. M. Nau, M. Olivucci. *Angew. Chem., Int. Ed.* **40**, 4185–4189 (2001); ibid. *Angew. Chem*. **22**, 4313 (2001).
3. A. Sinicropi, W. M. Nau, M. Olivucci. *Photochem. Photobiol. Sci.* **1**, 537–546 (2002).
4. N. Ismail, L. Blancafort, M. Olivucci, B. Kohler, M. A. Robb. *J. Am. Chem. Soc.* **124**, 6818 (2002).
5. M. Merchán and L. Serrano-Andrés. *J. Am. Chem. Soc.* **125**, 8108–8109 (2003).
6. M. Garavelli, C. S. Page, P. Celani, M. Olivucci, W. E. Schmid, S. A. Trushin, W. Fuss. *J. Phys. Chem. A* **105**, 4458–4469 (2001).
7. F. Bernardi, M. Olivucci, M. A. Robb. *Chem. Soc. Rev.* **25**, 321–328 (1996) and references cited therein.
8. F. Bernardi, M. Olivucci, J. Michl, M. A. Robb. *Spectrum* **9**, 1–6 (1996).
9. H. E. Zimmerman. *J. Am. Chem. Soc.* **88**, 1566 (1966).
10. H. E. Zimmerman. *Science* **153**, 837 (1966).
11. H. E. Zimmerman. *J. Am. Chem. Soc.* **88**, 1564 (1966).
12. J. Michl. *Mol. Photochem.* **4**, 243–255 (1972).
13. J. Michl. *Top. Curr. Chem.* **46**, 1 (1974).
14. L. Salem. *J. Am. Chem. Soc.* **96**, 3486–3501 (1974).
15. F. Bernardi, S. De, M. Olivucci, M. A. Robb. *J. Am. Chem. Soc.* **112**, 1737–1744 (1990).
16. F. Bernardi, M. Olivucci, M. A. Robb. *Acc. Chem. Res.* **23**, 405–412 (1990).
17. A. Migani and M. Olivucci (Eds.). In *Conical Intersections: Electronic Structure, Dynamics and Spectroscopy*, World Scientific, Singapore (2004).
18. R. Tsien. *Annu. Rev. Biochem.* **67**, 510 (1998).
19. M. Zimmer. *Chem. Rev.* **102**, 759–781 (2002).
20. R. A. Mathies and J. Lugtenburg (Eds.). In *Handbook of Biological Physics*, Vol. 3, Elsevier, Amsterdam (2000).
21. H. Kandori, Y. Shichida, T. Yoshizawa. *Biochemistry (Moscow)* **66**, 1197–1209 (2001).
22. D. Mandal, T. Tahara, N. M. Webber, S. R. Meech. *Chem. Phys. Lett.* **358**, 495–501 (2002).
23. N. M. Webber, K. L. Litvinenko, S. R. Meech. *J. Phys. Chem. B* **105**, 8036 (2001).
24. M. Chattoraj, B. A. King, G. U. Bublitz, S. G. Boxer. *Proc. Natl. Acad. Sci. USA* **93**, 8362 (1996) and references therein.
25. C. S. Page and M. Olivucci. *J. Comput. Chem.* **24**, 298–309 (2003).

26. W. D. Cornell, P. Cieplak, C. I. Bayly, I. R. Gould, K. M. Merz, Jr., D. M. Ferguson, D. C. Spellmeyer, T. Fox, J. W. Caldwell, P. A. Kollman. *J. Am. Chem. Soc.* **117**, 5179–5197 (1995).
27. A. D. MacKerell, Jr., D. Bashford, M. Bellott, R. L. Dunbrack, Jr., J. Evanseck, M. J. Field, S. Fischer, J. Gao, H. Guo, S. Ha, D. Joseph, L. Kuchnir, K. Kuczera, F. T. K. Lau, C. Mattos, S. Michnick, T. Ngo, D. T. Nguyen, B. Prodhom, W. E. Reiher III, B. Roux, M. Schlenkrich, J. Smith, R. Stote, J. Straub, M. Watanabe, J. Wiorkiewicz-Kuczera, D. Yin, M. Karplus. *J. Phys. Chem. B* **102**, 3586–3616 (1998).
28. N. Ferré and M. Olivucci. *J. Am. Chem. Soc.* **125**, 6868–6869 (2003).
29. N. Ferré and M. Olivucci. *THEOCHEM* **632**, 71–82 (2003).
30. U. C. Singh and P. A. Kollman. *J. Comput. Chem.* **7**, 718 (1986).
31. T. Vreven and K. Morokuma. *Theor. Chem. Acc.* **109**, 125–132. (2003).
32. S. Hayashi, E. Tajkhorshid, K. Schulten. *Biophy. J.* **83**, 1281–1297 (2002).
33. G. Groenhof, M. Bouxin-Cademartory, B. Hess, S. P. de-Visser, H. J. C. Berendsen, M. Olivucci, A. E. Mark, M. A. Robb. *J. Am. Chem. Soc.* **126**, 4228–4233 (2004).
34. A. Toniolo, G. Granucci, T. J. Martinez. *J. Phys. Chem. A* **107**, 3822–3830 (2003).
35. A. Toniolo, S. Olsen, L. Manohar, T. J. Martinez. *Faraday Discuss.* **127**, 149–163 (2004).
36. A. Warshel and Z. T. Chu. *J. Phys. Chem. B* **105**, 9857–9871 (2001).
37. A. Warshel and M. Levitt. *J. Mol. Biol.* **103**, 227–249 (1976).
38. S. Hayashi, E. Tajkhorshid, K. Schulten. *Biophys. J.* **85**, 1440–1449 (2003).
39. A. Warshel, Z. T. Chu, J.-K. Hwang. *Chem. Phys. Lett.* **158**, 303–314 (1991).
40. M. E. Martin, F. Negri, M. Olivucci. *J. Am. Chem. Soc.* **126**, 5452–5464 (2004).
41. A. Sinicropi, T. Andruniow, N. Ferré, R. Basosi, M. Olivucci. Submitted for publication.
42. T. Andruniow, N. Ferré, M. Olivucci. *Proc. Natl. Acad. Sci. USA* **101** (52), 17908–17913 (2004).
43. A. Migani, A. Sinicropi, N. Ferré, A. Cembran, M. Garavelli, M. Olivucci. *Faraday Discuss.* **127**, 179–191 (2004).
44. I. Wilner. *Acc. Chem. Res.* **30**, 347–356 (1997).
45. H. Kessler. *Angew. Chem., Int. Ed. Engl.* **21**, 512–523 (1982).
46. H. R. Haubner, D. Finsinger, H. Kessler. *Angew. Chem., Int. Ed. Engl.* **36**, 1375– 1389 (1997).
47. L. Ulysse, J. Cubillos, J. Chmielewski. *J. Am. Chem. Soc.* **117**, 8466–8467 (1995) .
48. R. Behrendt, C. Renner, M. Schenk, F. Wang, J. Wachtveitl, D. Oesterhelt, L. Moroder. *Angew. Chem., Int. Ed. Engl.* **38**, 2771–2774 (1999).
49. C. Renner, R. Behrendt, S. Sporlein, J. Wachtveitl, L. Moroder. *Biopolymers* **54**, 489–500 (2000).
50. J. Helbing, H. Bregy, J. Bredenbeck, R. Pfister, P. Hamm, R. Huber, J. Wachtveit, L. D. Vico, M. Olivucci. *J. Am. Chem. Soc.* **126**, 8823–8824 (2004).
51. T. Andruniow, S. Fantacci, F. D. Angelis, M. Olivucci. (2005). Submitted for publication.
52. D. S. Ruiz, A. Migani, A. Pepi, E. Busi, R. Basosi, L. Latterini, F. Elisei, S. Fusi, F. Ponticelli, V. Zanirato, M. Olivucci. *J. Am. Chem. Soc.* **126**, 9349–9359 (2004).